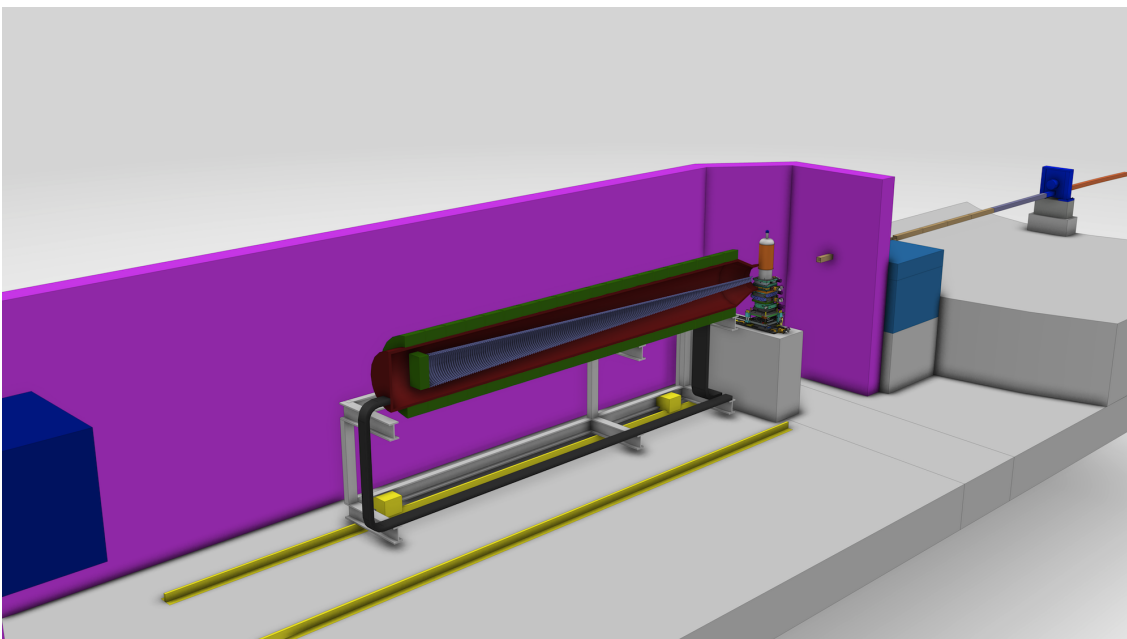


# ESS Construction Proposal

## LoKI - A broad-band SANS instrument



### **Proposers**

Dr. Andrew J Jackson, *ESS & Lund University, Sweden*

Dr. Kalliopi Kanaki, *ESS, Sweden*

### **Scientific Partners**

Prof. Lise Arleth, *Copenhagen University, Denmark*

Dr. Joachim Kohlbrecher, *Paul Scherrer Institute, Switzerland*

Prof. Adrian Rennie, *Uppsala University, Sweden*



## Executive Summary

Small angle neutron scattering is a technique that is applied across a spectrum of scientific disciplines, with users from chemistry, physics, biology, materials science, engineering and geoscience. LoKI is designed primarily with the needs of the soft matter, biophysics and materials science communities in mind and the trend in all of these fields is towards complexity and heterogeneity.

Complexity manifests itself in the study of multi-component systems studied as a function of multiple environmental conditions (e.g. pressure, temperature, shear, magnetic field) simultaneously. In order to be able to examine the possible parameter space, a combination of faster measurements, measurements on smaller sample volumes, and measurements with good signal-to-noise is required.

Heterogeneity is seen both spatially and temporally. Spatial heterogeneity is manifested as different structure at different length scales, from the nanometre scale to the millimetre scale. This can be driven by applied stimuli such as shear, flow, electrical or magnetic fields, or by intrinsic structural features of the material. Examples of the former are shear banding in surfactant systems and the flow re-orientation of polymers. Examples of the latter are nano-composite materials, multi-component gels, and porosity in rocks. To address this spatial heterogeneity requires a wide Q range to examine the sub-micrometre length scales and small beams to examine the heterogeneity on the millimetre scale. Furthermore, since these heterogeneities are often driven by non-equilibrium conditions, the accessible Q range must be measured simultaneously. Temporal heterogeneity is seen in the form of stimulus-response experiments (e.g. shear relaxation), in the kinetics of formation of materials when the components of the material are mixed (e.g. mixed micelle formation) and in the growth of biomolecule aggregates such as fibrils. In order to examine these systems with sufficient time resolution a high neutron flux is required and a wide simultaneous Q range is needed.

Not only are the systems of interest becoming more complex and heterogeneous, but they are also becoming smaller in volume. Examples of this are the small amounts of protein complexes that can be purified and deuterated, thin film systems such as organic photovoltaics, and bio-mimetic or polymer membranes.

The ability to reach Q values above the typical 0.8 to 1.0  $\text{\AA}^{-1}$  opens up significant areas of new science when combined with wide-angle scattering studies and the rapidly advancing fields of materials simulation. The study of, for example, ionic liquids and their ordering in the presence of solutes calls for the combination of SANS, wide-angle scattering and atomistic or coarse-grained molecular dynamics simulations. The analysis techniques used in biological solution scattering, such as ab-initio shape reconstruction, require data out to high Q as do studies of nano-composite materials where the size of the particles or domains may be only a few nanometres.

LoKI is designed to address these needs by providing a high flux - at least 10 times the current leading reactor based instrument - and a broad simultaneous Q range of at least three orders of magnitude. This is achieved by the choice of instrument length (10m collimation + 10m sample to detector distance instrument with the sample position 20 m from the moderator) and a large solid angle of detector coverage.

Whilst some of the types of experiment mentioned above are done at present, they are often tour-de-force studies pushing the capabilities of today's instruments. LoKI will provide a world leading combination of high neutron flux and wide simultaneous Q range with the ability to study smaller samples and with these characteristics, LoKI will enable scientists to answer the challenging materials science questions of tomorrow in fields from health and aging, to sustainability and energy security.

# Contents

<b>1</b>	<b>Scientific Impact</b>	<b>1</b>
<b>2</b>	<b>User Base and Demand</b>	<b>3</b>
<b>3</b>	<b>Description of Instrument Concept and Performance</b>	<b>5</b>
3.1	Introduction . . . . .	5
3.2	Instrument Objectives . . . . .	5
3.3	Instrument Overview . . . . .	6
3.4	Beam Delivery . . . . .	6
3.5	Sample Area . . . . .	12
3.6	Detectors . . . . .	12
3.7	Estimates of Instrument Performance . . . . .	15
<b>4</b>	<b>Strategy and Uniqueness</b>	<b>21</b>
<b>5</b>	<b>Technical Maturity</b>	<b>23</b>
5.1	Location . . . . .	23
5.2	Risk Management . . . . .	23
<b>6</b>	<b>Costing</b>	<b>27</b>

# 1 Scientific Impact

Small angle neutron scattering is a technique that is applied across a spectrum of scientific disciplines, with users from chemistry, physics, biology, materials science, engineering and geoscience. LoKI is designed primarily with the needs of the soft matter, biophysics and materials science communities in mind and the trend in all of these fields is towards complexity and heterogeneity.

Complexity manifests itself in the study of multi-component systems studied as a function of multiple environmental conditions (e.g. pressure, temperature, shear, magnetic field) simultaneously. In order to be able to examine the possible parameter space, a combination of faster measurements, measurements on smaller sample volumes, and measurements with good signal-to-noise is required.

Heterogeneity is seen both spatially and temporally. Spatial heterogeneity is manifested as different structure at different length scales, from the nanometre scale to the millimetre scale. This can be driven by applied stimuli such as shear, flow, electrical or magnetic fields, or by intrinsic structural features of the material. Examples of the former are shear banding in surfactant systems and the flow re-orientation of polymers. Examples of the latter are nano-composite materials, multi-component gels, and porosity in rocks. To address this spatial heterogeneity requires a wide  $Q$  range to examine the sub-micrometre length scales and small beams to examine the heterogeneity on the millimetre scale. Furthermore, since these heterogeneities are often driven by non-equilibrium conditions, the accessible  $Q$  range must be measured simultaneously.

Temporal heterogeneity is seen in the form of stimulus-response experiments (e.g. shear relaxation), in the kinetics of formation of materials when the components of the material are mixed (e.g. mixed micelle formation) and in the growth of biomolecule aggregates such as fibrils. In order to examine these systems with sufficient time resolution a high neutron flux is required and a wide simultaneous  $Q$  range is needed.

Not only are the systems of interest becoming more complex and heterogeneous, but they are also becoming smaller in volume. Examples of this are the small amounts of protein complexes that can be purified and deuterated, thin film systems such as organic photovoltaics, and bio-mimetic or polymer membranes. In these cases it is vital that the instrumental background be as low as possible in order to discern the small scattering signal obtained.

Through the use of neutron event recording, which identifies the time of arrival of each neutron at the detector, LoKI will allow the scientist to make this decision on the fly and variably as a function of  $Q$ . This is valuable for materials such as block-copolymer blends where there are strong peaks in the data that require high resolution but the inter-peak scattering is of lower intensity and so requires more neutron counts but can make use of lower resolution. In particular there is a need to have good  $Q$  resolution at high  $Q$ , for example in studies of fibres, liquid crystals or multi-lamellar systems such as lipid or surfactant vesicles. The ability to make use of longer wavelength, higher time resolution, neutrons at high angles will be key to being able to make use of post-measurement resolution tuning. This requirement demands a large solid angle of detectors and thus potentially a large area detector close to the sample.

The ability to reach  $Q$  values above the typical  $0.8$  to  $1.0 \text{ \AA}^{-1}$  opens up significant areas of new science when combined with wide-angle scattering studies and the rapidly advancing fields of materials simulation. The study of, for example, ionic liquids and their ordering in the presence of solutes calls for the combination of SANS, wide-angle scattering and atomistic or coarse-grained molecular dynamics simulations. The analysis techniques used in biological solution scattering, such as ab-initio shape reconstruction, require data out to high  $Q$  as do

studies of nano-composite materials where the size of the particles or domains may be only a few nanometres.

Non-equilibrium studies often use complex sample environment and require strong integration of the sample environment with the neutron measurement in order to tie sample conditions tightly to the measured scattering. Space is also required for the use of in-situ complementary measurement techniques, for example light or x-ray scattering, or UV spectroscopy simultaneously with the neutron scattering measurement. LoKI has a flexible sample area that can be easily re-tooled for different experiments through the use of interchangeable sample environment platforms.

Whilst some of the types of experiment mentioned above are done at present, they are often tour-de-force studies pushing the capabilities of today's instruments. LoKI provides a world leading combination of high neutron flux and wide simultaneous Q range with the ability to study small samples.

With these characteristics, LoKI will enable scientists to answer the challenging materials science questions of tomorrow in fields from health and aging, to sustainability and energy security.

## 2 User Base and Demand

The community of small angle scattering users is large in number and covers a wide range of scientific disciplines. Demand for access to SANS beamtime is high, with major scattering centres regularly having oversubscription levels of 3 or more. It is indicative of the demand that as more SANS instruments have been built, oversubscription has remained high.

SANS produces between 500 and 600 papers annually, with the breakdown by discipline shown in figure 1. The most productive area for small angle scattering is in materials and polymer science, matching the mission of the ESS to be at the forefront of research in materials science. The second largest area is chemistry, the bulk of which is studies on colloid and surfactant systems. Thus an instrument such as LoKI will address at least 60 % of the existing user community. The increased flux and simultaneously accessible Q range of LoKI will enable studies on cutting edge materials under real world conditions that have not previously been possible due to limitations in signal-to-noise and measurement time.

Simplicity of operation, including integration of sample environment and automated data reduction, will make the instrument accessible to new and infrequent users, with most being able to simply load their samples and press "Run". This, combined with the advantages listed above, will allow development of new user communities from the food science and biotechnology industries and expansion of usage by the biology and biophysics communities.

It is expected that demand for beamtime on LoKI will be high and once the ESS is fully operational in 2025, the instrument will host up to 120 experiments a year.

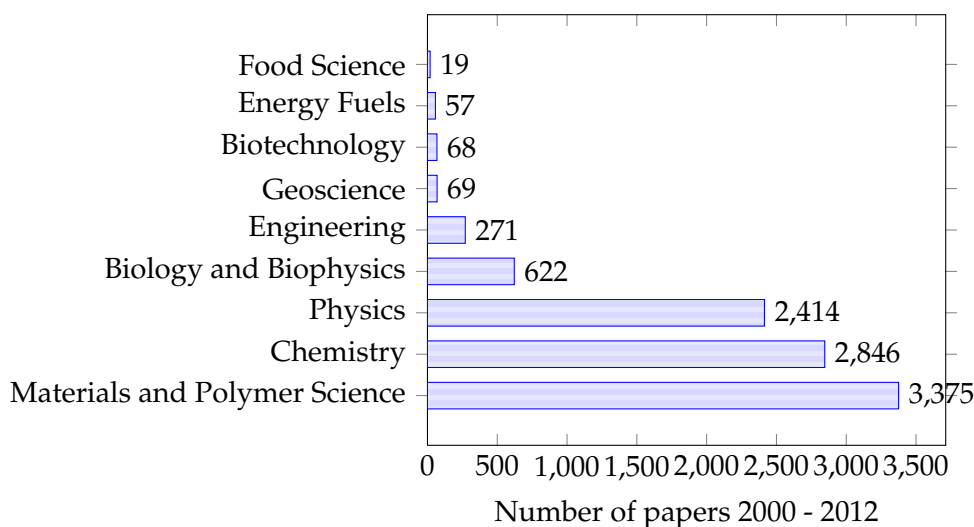


Figure 2.1: SANS publications by research field 2000-2012 (data from Thompson Reuters ISI Web of Science)





## 3 Description of Instrument Concept and Performance

### 3.1 Introduction

In order to maximise the utility of the instantaneous flux that will be available at the ESS, it is important to design SANS instruments that can use the whole pulse and access as wide as possible a Q range in a single measurement. Indeed, the SANS STAP has recommended that three orders of magnitude in Q simultaneously should be our target. Historically, SANS instruments at reactor sources have had variable collimation and moveable detectors to enable a wide Q range to be examined. There is now a trend towards using multiple detector banks to access more scattering angle at the same time and this proposal considers such a method in extremis with a novel detector geometry using new detector technologies based on  $^{10}\text{B}$  thin film systems.

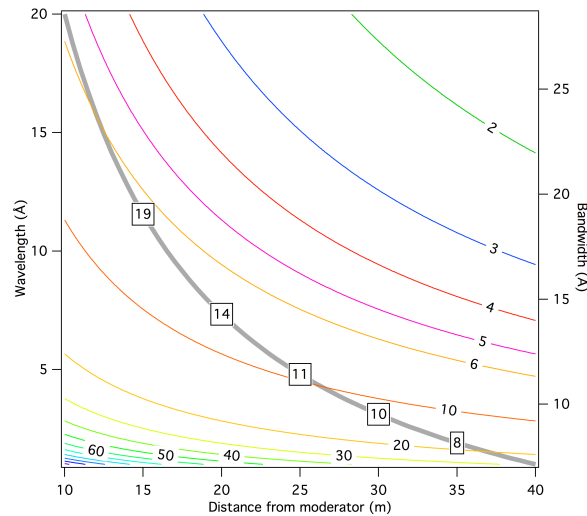


Figure 3.1: Time Resolution as a function of wavelength (contours) and maximum Bandwidth at a given distance from the source (grey line, right hand scale)

Figure 2 shows the time resolution and bandwidth as a function of distance from the moderator at ESS. In order to access the maximum possible Q range, ideally we would place our detectors close to the source in order to maximise the accessible bandwidth. However this comes at the cost of rather poor resolution, even for SANS, and tight space constraints. Thus we balance the bandwidth with resolution and space requirements for sample environment. The primary focus, however, is maximising simultaneously accessible Q.

In order to achieve a very broad dynamic Q range, a large solid angle of detectors is required and to this end, two options for detector layout are presented.

### 3.2 Instrument Objectives

- 1) Broad simultaneous Q range:  $Q < 1 \times 10^{-3} \text{ \AA}^{-1}$  to  $Q > 1 \text{ \AA}^{-1}$  with pinhole collimation geometry.
- 2) High flux making maximum use of the high source brightness at the ESS.
- 3) Flexible sample area to allow for a variety of sample environment equipment.
- 4) Simplicity of operation for non-experts including automated data reduction.

### 3.3 Instrument Overview

LoKI has a maximum sample-to-detector distance of 10 m and a maximum collimation length of 10 m. This is dictated by the balance of bandwidth and achieving a sufficiently low angle of scattering. Once space for the initial optical components has been included, this leads to a maximum source-to-detector distance of 30 m.

The instrument will therefore have an overall length (moderator to back of detector tank) of up to 40m including shielding. Figure 3.2 shows the baseline layout of the instrument.

The instrument will have two operation modes:

Mode 1: A chopper is used running at the source frequency. This mode provides for operation across the frame boundary and provides the maximum bandwidth whilst avoiding frame overlap.

Mode 2: The same chopper as Mode 1 is used but running at half the source frequency. This mode provides for measurement across two source frames and doubles the bandwidth compared to Mode 1.

### 3.4 Beam Delivery

The guide size is 3 cm x 3 cm throughout the whole instrument.

#### Bender

A bender is used to avoid line-of-sight to the moderator and also acts as a short wavelength cut-off filter. In order to get twice out of line-of-sight and to keep the bender within the monolith, the radius must be 78 m and the length 4 m (Figure 3.3). In addition to obtaining an offset of twice line-of-sight at the sample position, the bender gives more than one times line-of-sight offset at the start of the collimation section.

Simulations of bender transmission (Figure 3.4) show that 4 channels with an  $m=4$  coating provide greater than 80% of the transmission of a straight  $m=4$  guide above  $4\text{\AA}$ , and greater than 80% of the transmission of a straight  $m=1$  guide above  $2\text{\AA}$ .

The increases in transmission seen for an  $m=4$  over that of an  $m=3$  bender could be the result of simply transporting higher divergence neutrons that will not be useful in the instrument. Figure 3.5 shows the vertical and horizontal divergence at the end of the bender as a function of wavelength and guide coating. The maximum useable divergence is  $\pm 0.4^\circ$  in each direction and the white boxes thus show the useable neutrons. We can see that  $m=3$  is clearly better than  $m=2$  in both directions and that  $m=4$  is transporting more high divergence neutrons outside the useable range than  $m=3$  as expected. However, this may be a reasonable trade-off as the useful range is better filled at  $m=4$ , at least in terms of the horizontal divergence.

#### Wavelength Band Selection

Wavelength selection and frame overlap prevention is performed using two double-disc choppers. The first chopper, located at 6.5 m from the source, has two co-rotating discs, each with a  $120^\circ$  opening. This provides for an adjustable chopper aperture through variation of the phasing between the two discs. The second chopper, located at 9.8 m from the source, is identical to the first and provides the frame overlap prevention.

As introduced above, LoKI provides two modes of operation offering different wavelength bands and hence different Q ranges.

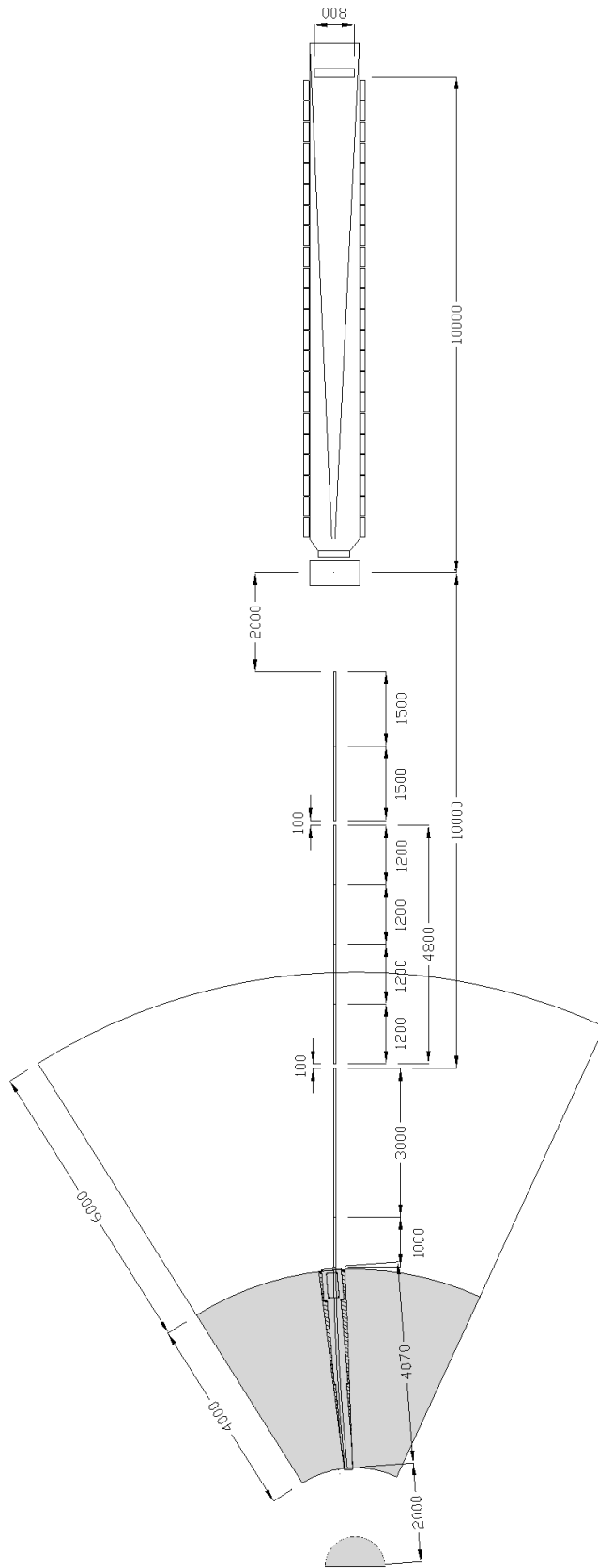


Figure 3.2: Baseline instrument layout (to scale, dimensions in mm)

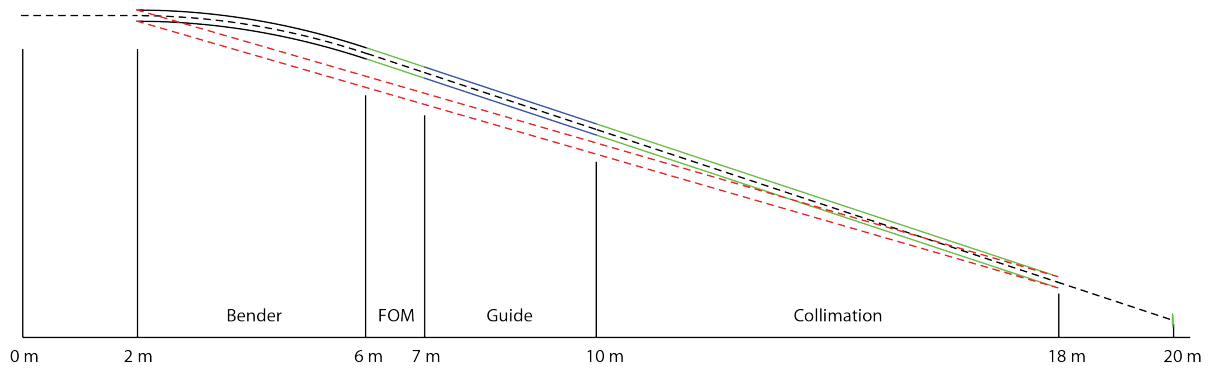


Figure 3.3: Top view of the guide system showing avoidance of line-of-sight using 4m long bender

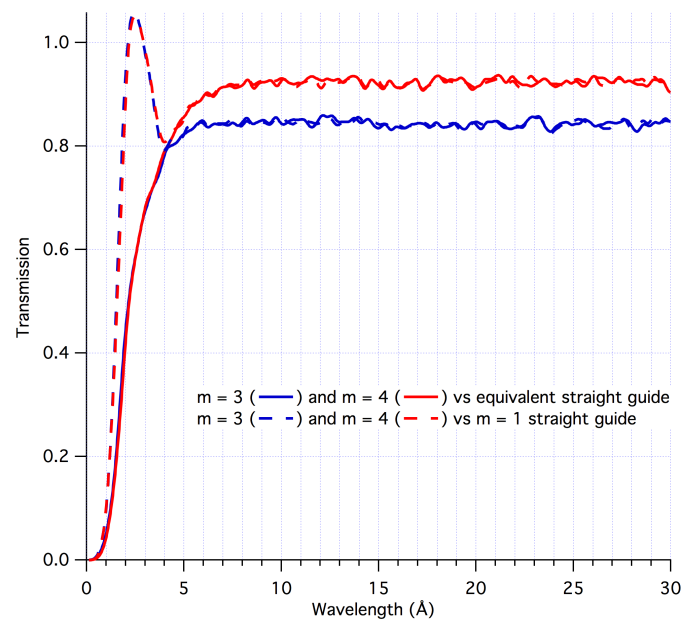


Figure 3.4: Simulated bender transmission for  $m = 3$  and  $m = 4$  multi-channel benders.

Mode 1 has the choppers running at 14 Hz. To access the wavelength band from  $3 \text{ \AA}$  to  $10.5 \text{ \AA}$  ( $1.8 \text{ \AA}$  to  $11.6 \text{ \AA}$  with penumbra), an open time of 15.16 ms is required as seen in Figure 3.6. The timing of the chopper with respect to the source can be adjusted such that different ranges of wavelength can be selected. Such an offset is shown in Figure 3.7 where  $10.5 \text{ \AA}$  to  $18.0 \text{ \AA}$  ( $9.3 \text{ \AA}$  to  $19.1 \text{ \AA}$  with penumbra) neutrons are selected. This allows the scientist to select for lower  $Q$  values whilst still using every pulse from the source. Such operation will also improve the wavelength resolution, as longer wavelengths will be used.

Mode 2 has the choppers running at 7 Hz. This allows access to the wavelength band from  $3 \text{ \AA}$  to  $19.9 \text{ \AA}$  ( $1.8 \text{ \AA}$  to  $21.0 \text{ \AA}$  with penumbra), using every other source pulse as shown in Figure 3.8. In order to achieve this range whilst still completely filling the frame the open time of the choppers must be adjusted, by changing the phasing of the discs, to be longer than twice that of 14Hz operation.

### Prompt Pulse

Operating in Mode 2, where every other frame is skipped, means that whilst the choppers will block the cold neutrons from the source the fast neutrons in the prompt pulse will not

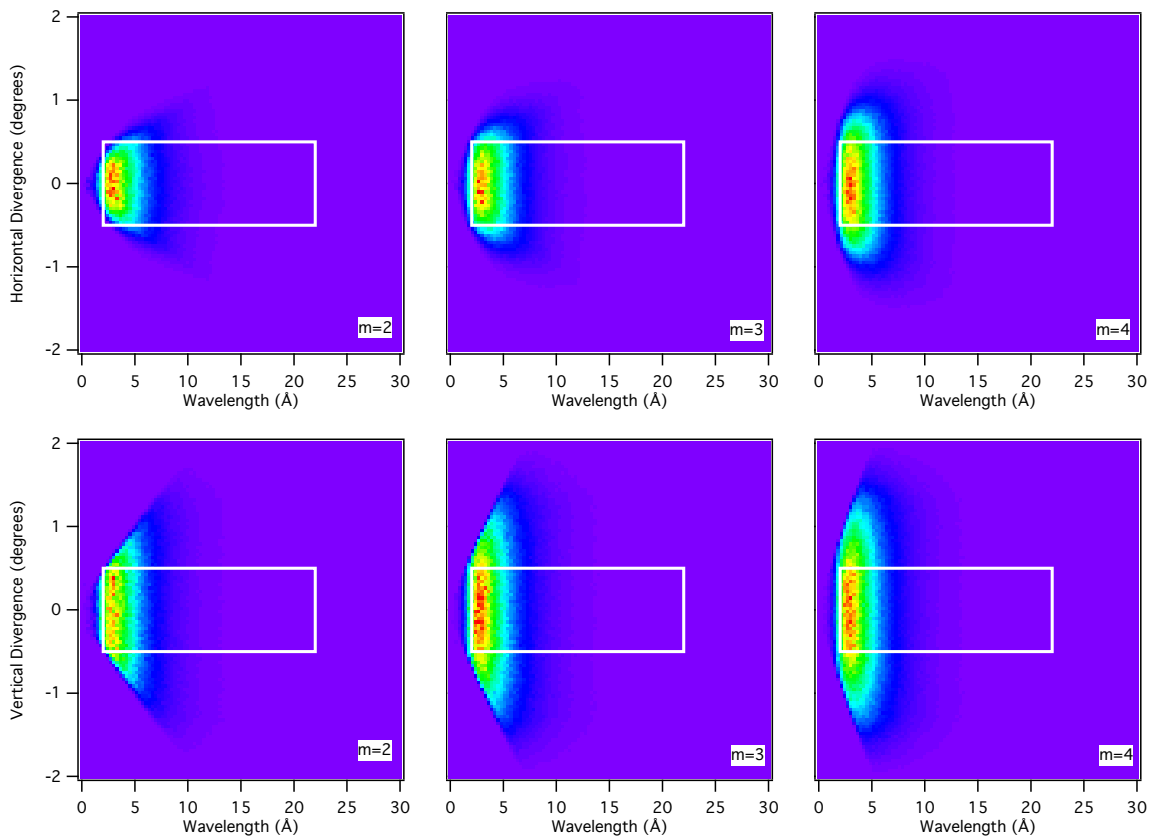


Figure 3.5: Simulated divergence at the bender exit for  $m = 2$ ,  $m = 3$  and  $m = 4$  multi-channel benders. The white box indicates the useable divergence-wavelength space.

be blocked. This could appear twice in every measurement frame as extraneous signal on the detectors, rendering up to 12 ms of the frame unusable as the prompt pulse is expected to extend beyond the nominal pulse width of 3 ms. The use of the bender to take the sample position twice out of line-of-sight from the moderator means that such neutrons should not reach the instrument directly down the guide. However, if the shielding is inadequate, the prompt signal may still appear. This requires study by the ESS target and instrument support divisions and is discussed further under Risk Management in section 5.

### Chopper Speed

Modes 1 and 2 both employ relatively slow choppers (840 rpm and 420 rpm respectively) and thus the amount of time it takes to open or close the guide as the chopper passes could be a problem. Using a 70 cm diameter chopper, the guide crossing time at 14 Hz is approximately 1.2 ms for a 3 cm guide. At 7 Hz it is twice that value, 2.4 ms. In each mode, this leads to a possible reduction in the minimum and maximum accessible wavelengths by introducing a small frame overlap which can be mitigated by simply rejecting events in the overlap range. This is not, however, a significant performance issue since the flux in the overlap region will be very low already.

### Guides and Collimation

Following the first chopper pair, there is a static section of  $m=1$  guide, extending to a position 9.6 m from the source, to restore uniformity to the distribution of neutrons over the guide exit.

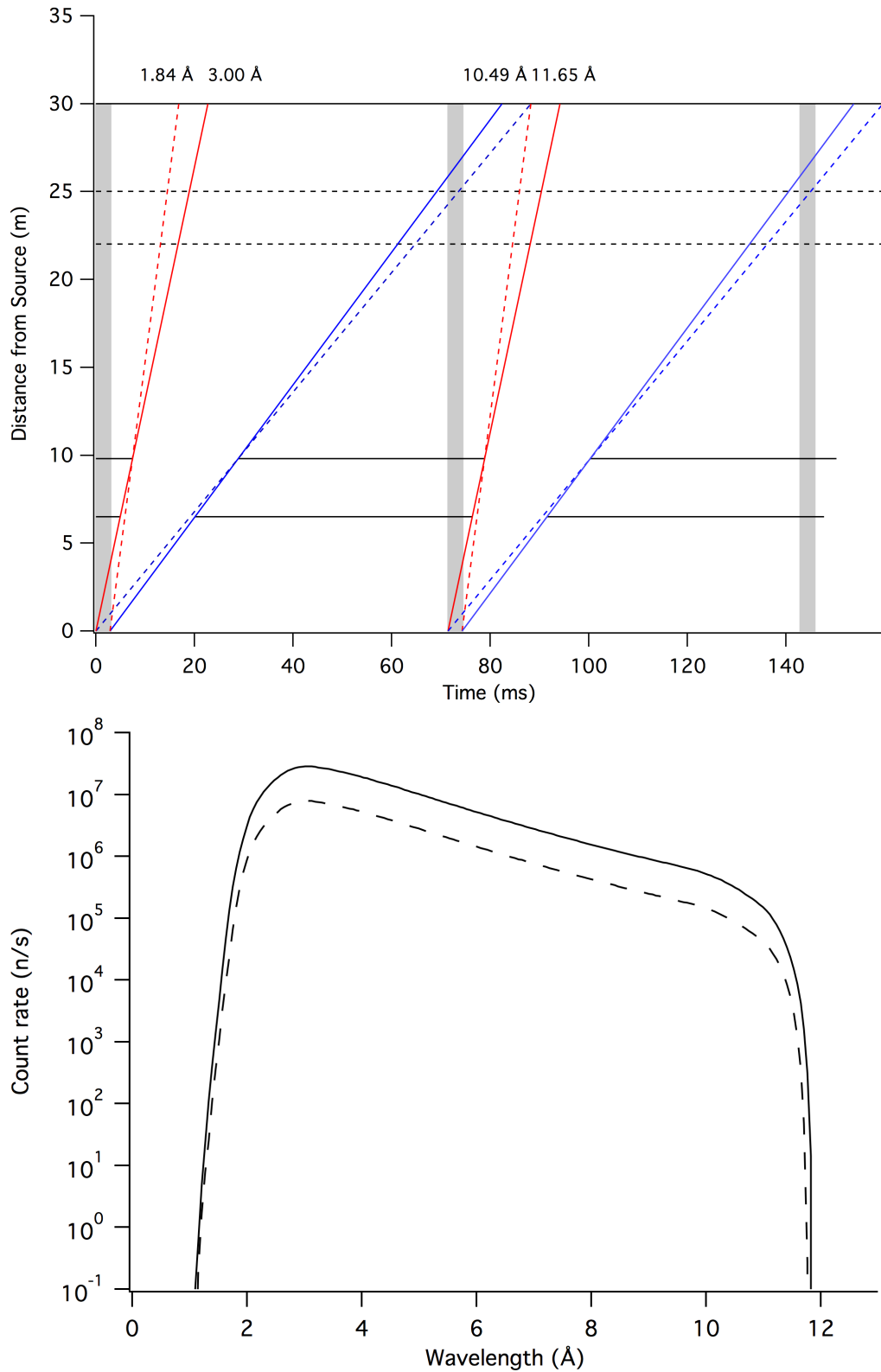


Figure 3.6: (top) Time-distance diagram showing the available wavelength band of 3 to 10.5 Å (1.8 to 11.6 Å) available in Mode 1. (bottom) Monte-carlo simulated spectrum at the sample position for 5m (solid line) and 10 m (dashed line) collimation.

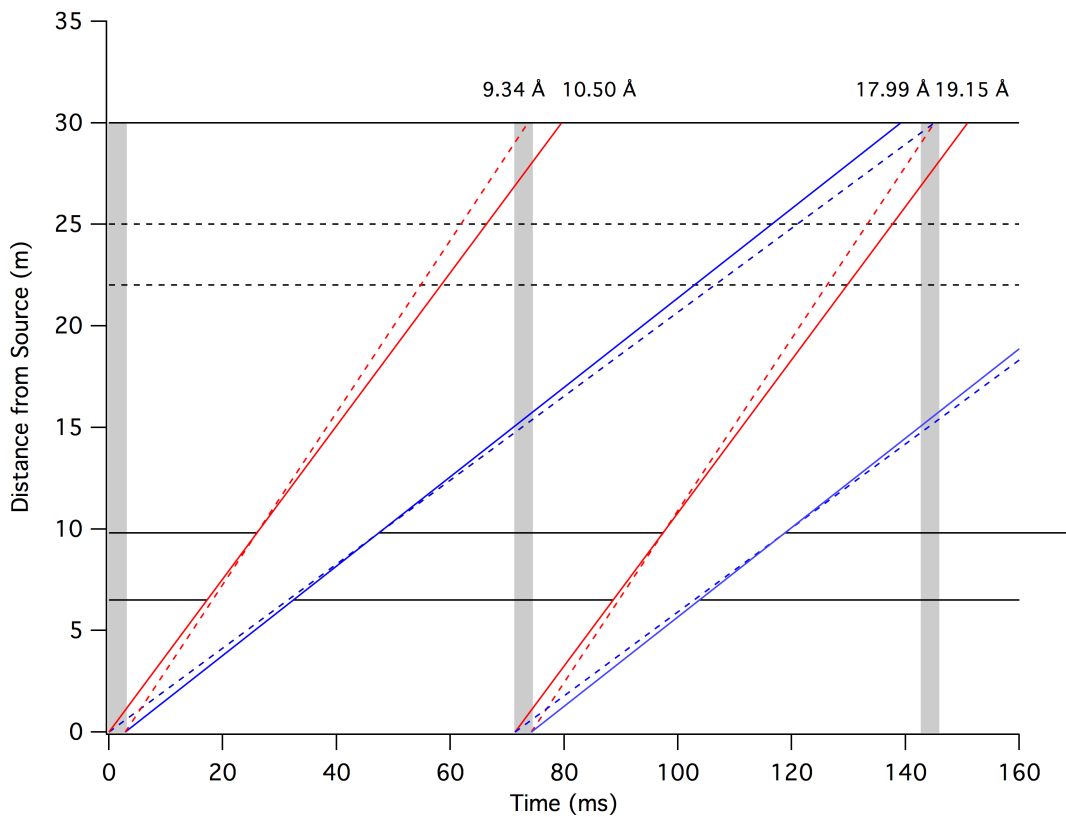


Figure 3.7: Time-distance diagram showing and alternative use of the choppers to give an available wavelength band of 10.5 to 18.0 Å (9.3 to 19.1 Å) available in Mode 1.

Collimation of the beam will be performed using apertures and two regions of automatically interchangeable guides. The interchangeable sections of guide will be 4.8 m long and 3 m long respectively (see figure 3.2). Automatically changeable apertures will be located at the start of the collimation section (10 m from source), after the first interchangeable section (15 m from source) just outside the common shielding bunker and after the second interchangeable guide section (18m from the source). A manually interchangeable evacuated flight path will be provided between the end of the guide at 18m and the sample position at 20m with different lengths available to accommodate different sample environment.

As part of the initial engineering design phase, the possibility of keeping the guides in place whilst having only the apertures change to adjust the collimation will be investigated.

### Optional Instrument Optics

The final 3m section of interchangeable guide and 2m of evacuated flight path is outside the heavy common shielding. It will thus have more space for possible additional components such as focussing optics in the form of magnesium fluoride lenses or concentric mirrors (Wolter optics). The study of the possibilities for using focussing optics to achieve lower Q with larger samples, and thus at higher flux, is ongoing.

This space between the end of the guide (at 18m) and the sample could also be used to house a set of SESANS coils to allow for simultaneous SANS and SESANS using a high resolution detector in the beamstop. It is desirable to measure the direct beam for normalisation of the data in any case (see section 3.6). In order to accommodate this option, it may be necessary for the detector vacuum vessel to move backwards to increase the space available. This option

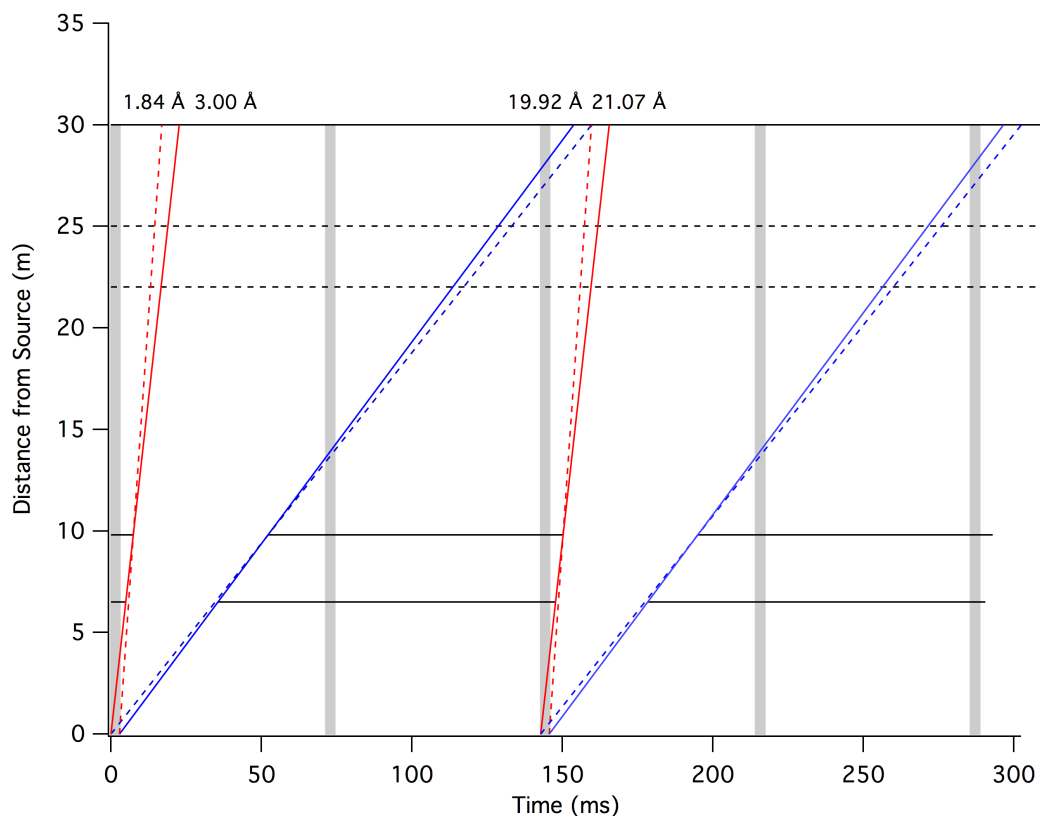


Figure 3.8: Time-distance diagram showing and alternative use of the choppers to give an available wavelength band of 3 to 19.9 Å (1.8 to 21.0 Å) available in Mode 1.

will be considered further during the engineering design phase in collaboration with the work unit on spin-echo SANS.

### 3.5 Sample Area

The sample area allows for the use of relatively large (up to 2 m along and 3 m perpendicular to the beam direction) sample environment.

A system of removable sample environment packages is used that can be set up off line and then inserted into position reproducibly (similar to the system used on SANS2D at ISIS). This allows for rapid changeover between users and simpler setup of sample environment given the likely limited access space at the sample position. This system is particularly valuable when setting up equipment such as rheometers and shear cells, where the sample apertures need to be carefully aligned with the gap in the cell. It also ensures that complex sample environment can be tested offline without it having to be dismantled again to insert it at the beam position.

### 3.6 Detectors

SANS instrument have for many years made use of  $^3\text{He}$  based area detectors or  $^3\text{He}$  based tubes placed to form area detectors. There is a worldwide shortage of  $^3\text{He}$  that is unlikely to improve and so alternative detector technologies are being developed in a collaboration between neutron scattering facilities. Whilst many of these new detectors look very promising, it will not be clear for at least a few years how well they perform in real world use.



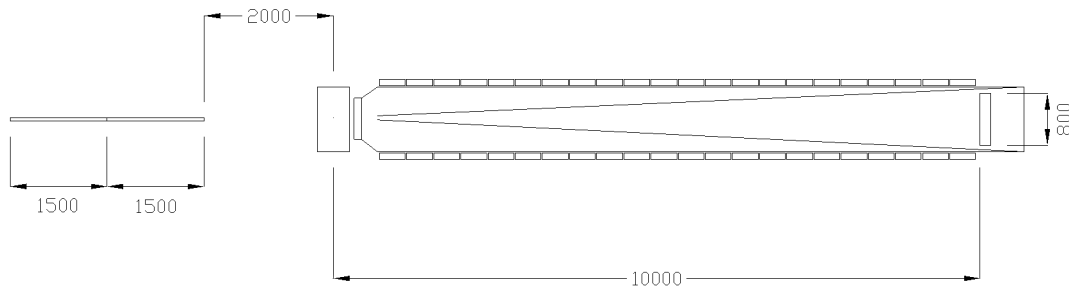


Figure 3.9: Layout of the proposed Boron-10 "lined tube" detector (to scale)

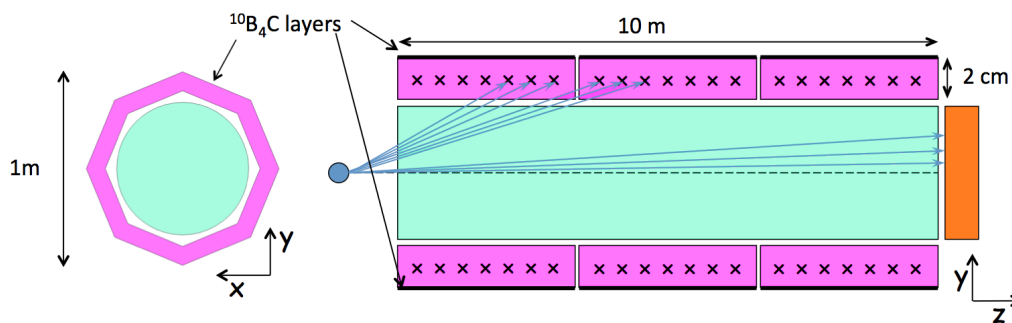


Figure 3.10: Detail of the proposed  $^{10}\text{B}$  "lined tube" detector.

Thus, two possible detector configurations that meet the scientific requirements are described. The final design of the instrument will use one of these based on the results of the initial engineering design phase and on the direction taken by developments in detector design and availability of technologies.

### "Lined Tube"

The baseline design of the instrument has a novel detector configuration making use of the characteristics of  $^{10}\text{B}$  thin film based detectors as shown in figures 10 and 11. Here  $^{10}\text{B}$  based detectors lie on the outside of a cylindrical vacuum vessel. The shallow angle that neutrons intersect the detector elements results in efficient capture of the neutron and high detection efficiency across the wavelength band of the instrument.

The detector elements are 10 cm wide by 40 cm long and have wires at 5 cm spacing running perpendicular to the beam direction. This provides good resolution along Q but relatively poor resolution perpendicular to Q. This is acceptable for azimuthally symmetric scattering that can be averaged to a 1 dimensional scattering curve, but is not suitable for studies of oriented systems where good azimuthal resolution is required. A second set of detection wires running along the beam direction, or a micro-strip type cathode readout, will provide the necessary azimuthal resolution for such studies.

A high resolution (2 mm or better) detector will be placed in the rear of the detector vessel and a scintillator based technology will most likely be used.

To avoid cross-talk between detectors across the detector vessel, a cone of neutron absorb-

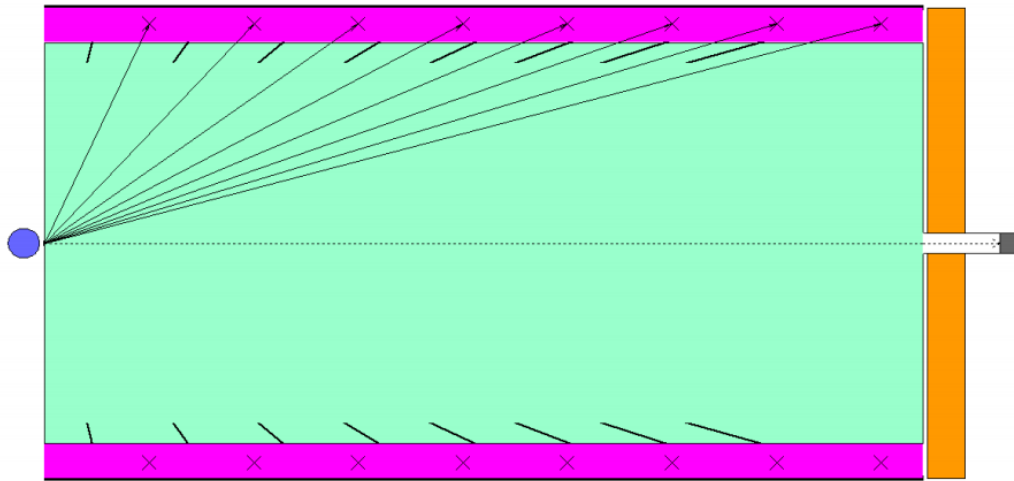


Figure 3.11: Possible scheme of cross-talk prevention and vessel strengthening through the inclusion of ribs running around the internal circumference of the vacuum tank between detection elements.

ing material (as shown in Figure 3.9) is mounted such that the rear detector is still viewable. Whilst there is a gap in measured angle, there is no gap in  $Q$  due to the wavelength band covered. The cone will be of a bellows type design to allow the rear detector to move along the beam axis within the vacuum vessel. This allows the optimum collimation to be maintained when the detector vessel is moved to accommodate sample environment. Alternatively, absorbing ribs will be fitted around the circumference of the tank to separate the detection elements as shown in Figure 3.11. This has the advantage that the ribs also act as stiffening for the vacuum vessel, allowing the walls to be thinner. These options will be explored in further detail during the initial engineering phase of construction.

### Energy Resolution

The efficiency of detection in  $^{10}\text{B}$  thin films varies with wavelength (Figure 3.12) and hence it may be possible to make use of multiple layers of films to perform coarse energy discrimination and hence accumulate neutrons in time-of-flight and energy histograms. Such a system has the potential to allow for the separation of inelastic incoherent scattering from the measured signal without requiring a reduction in incoming flux. This possibility is the subject of on-going studies with results due in March 2013. If such a system proves feasible, it could be easily implemented on the "lined tube" style detector system by adding a second layer of detection elements and tuning the thickness of the boron layer used in different parts of the detector array.

### "Window Frame"

The alternative layout has a "window frame" style of detector layout as seen in figure 3.13. The first detector has an area of 3 m x 3 m with a 1 m x 1 m window in the centre. The second detector has an area of 2.4 m x 2.4 m with a 0.4 m x 0.4 m window in the centre. The rear detector has an area of 0.5 m x 0.5 m.

The first two sets of detectors are fixed, whilst the rear detector can move forward on a carriage to match the 5 m collimation setting if the lowest  $Q$  is not required. All of the detectors sit inside a common vacuum vessel with a rectangular cross section.

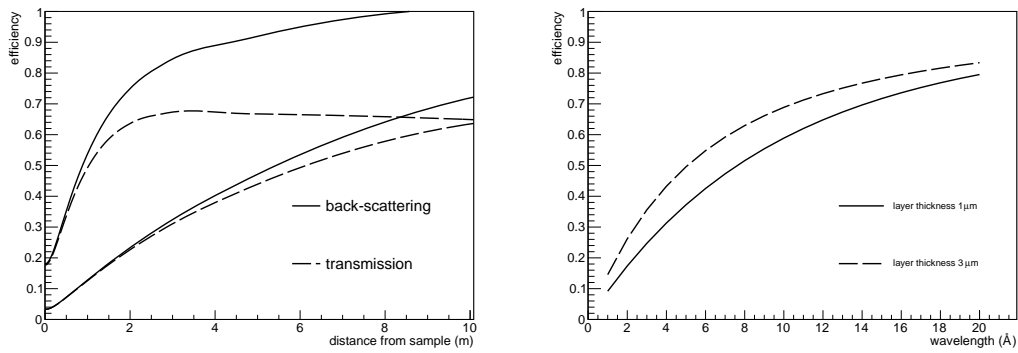


Figure 3.12: (left) Efficiency of a single layer of  $^{10}\text{B}$  as a function of distance along the "lined tube" detector at  $2 \text{ \AA}$  and  $12 \text{ \AA}$ . (right) Efficiency of a single  $1 \mu\text{m}$  or  $3 \mu\text{m}$  layer of  $^{10}\text{B}$  as a function of wavelength

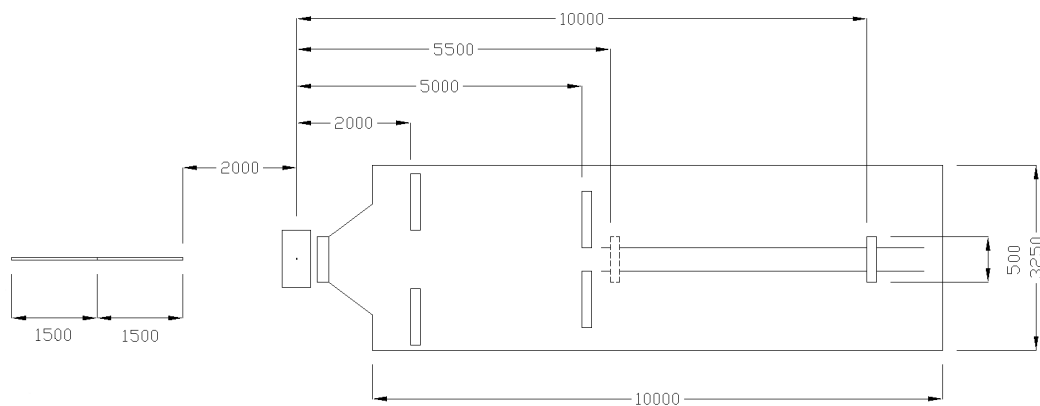


Figure 3.13: Layout of the proposed "window frame" detectors (to scale)

The technology used for the detectors is expected to be  $^{10}\text{B}$  based for the first two, lower resolution detectors, with an alternative such as anger cameras used for the rear, high-resolution detector. The front detectors will require a resolution of 8 mm or better and the rear detector will require a resolution of 2 mm or better. The first two detector banks could also be implemented using  $^3\text{He}$  tubes.

### Beamstop

In order to make transmission measurements without requiring beam attenuation, the beam-stops will be instrumented with detectors capable of providing a time-of-flight spectrum.

## 3.7 Estimates of Instrument Performance

### Q Range and Resolution

The size of aperture used and the spread of wavelengths determine the Q resolution, with larger beam sizes on the detector giving poorer angular resolution. The Q resolution in SANS can be defined in the simplest case as (Mildner and Carpenter 1984)

Distance (m)	Wavelength (Å)	Time-fo-flight (ms)	$\Delta t/t$
22	2	11.1	0.27
	12	66.7	0.05
25	2	12.6	0.24
	12	69.5	0.04
30	2	22.8	0.13
	12	68.3	0.04

Table 3.1: Time-of-flight resolution as a function of wavelength and source to detector distance

$$(\sigma_Q)^2 = k^2 \left[ \frac{R_1^2}{4L_1^2} + \frac{R_2^2}{4L_2^2} + \frac{(\delta R)^2}{12L_2^2} + \frac{R^2}{4L_2^2} \left( \frac{\delta \lambda}{\lambda} \right) \right] \quad (3.1)$$

where  $R_1$  and  $R_2$  are the radii of the source and sample apertures,  $L_1$  and  $L_2$  are the source-to-sample and sample-to-detector distances respectively,  $1/L' = 1/L_1 + 1/L_2$ ,  $R$  is the radial distance from the beam centre and  $\Delta R$  is the width of the azimuthal averaging ring.

The instruments at the ESS will all operate with event mode data recording i.e. each neutron event will be recorded with a time stamp related to the accelerator clock such that the time-of-flight of each neutron may be calculated. The uncertainty in arrival time at the detector will be dominated by the pulse length giving a  $\Delta t$  of  $\sim 3$  ms. Thus the uncertainty in wavelength will vary with wavelength and with distance from the source. It will therefore be possible to make decisions about trade offs in counting statistics and resolution after the fact during data reduction, where variable binning schemes will be possible.

To discuss the resolution, therefore, we should examine the possible limiting cases. As an example, Table 3.1 shows the time-of-flight for the lower and upper ends of the wavelength band used at each detector distance in the window frame configuration operated in Mode 1. The balance of contributions to the resolution determines the detector resolution required.

In order to calculate  $Q$  ranges, the traditional optimum SANS collimation has been used where the source aperture ( $Ap_1$ ) is twice the diameter of the sample aperture ( $Ap_2$ ). The accessible  $Q$  ranges are given based on the "full-flux" bandwidth as defined and shown in section 3.4 and thus represent a conservative estimate since there will still be significant numbers of short wavelength neutrons in the penumbra of the chopper. The minimum  $Q$  reported here is that at 1.5 times the beam radius on the rear detector.

Table 3.2 gives the  $Q$  range accessible in mode 1 for the "line tube" style detector and Table 3.3 gives those for the "window frame" style detector.

Thus we can see that either of the detector options will provide the 3 orders of magnitude in  $Q$  required, however the "window frame" style of detector provides a broader  $Q$  range and accesses the  $Q$  range above  $1 \text{ \AA}^{-1}$ . The "lined tube" style detector could be made wider in diameter or perhaps flared close to the sample in order to access higher  $Q$  values. Such options are under investigation.

## Neutron Beam Intensity

In order to estimate the performance of the instrument in terms of neutron count rates at the sample and on the detectors, monte carlo simulations have been performed including the full front end of the instrument consisting of:

**Bender** 4m long, 4 channels,  $m=4$  coating on all surfaces, 78 m radius of curvature

Ap2 Diam (mm)	L1 (m)	L2 (m)	$Q_{min}(\times 10^{-3} \text{ \AA}^{-1})$	$Q_{max} (\text{ \AA}^{-1})$	$Q_{max}/Q_{min}$
10	2	5	7.63	0.98	128
5	2	5	3.82	0.98	256
4	2	5	1.53	0.98	640
10	5	5	3.59	0.98	272
5	5	5	1.79	0.98	547
4	5	5	0.72	0.98	1361
10	10	10	1.79	0.98	547
5	10	10	0.90	0.98	1089
4	10	10	0.36	0.98	2722

Table 3.2: Accessible Q range for the "lined tube" detector in Mode 1 with a wavelength range of 3 Å to 10.5 Å

Ap2 Diam (mm)	L1 (m)	L2 (m)	$Q_{min}(\times 10^{-3} \text{ \AA}^{-1})$	$Q_{max} (\text{ \AA}^{-1})$	$Q_{max}/Q_{min}$
10	2	5	7.63	1.66	218
5	2	5	3.82	1.66	435
4	2	5	1.53	1.66	1085
10	5	5	3.59	1.66	462
5	5	5	1.79	1.66	927
4	5	5	0.72	1.66	2305
10	10	10	1.79	1.66	927
5	10	10	0.90	1.66	1844
4	10	10	0.36	1.66	4611

Table 3.3: Accessible Q range for the "window frame" detector in Mode 1 with a wavelength range of 3 Å to 10.5 Å

**Choppers** Positioned at 6.5m and 9.8m with a 40 cm guide break at each position

**Guides** m=1 coating, guide break for aperture at 10 m (extra space after chopper)

**Apertures** Source aperture set to twice radius of sample aperture. Sample aperture set to 10 mm and 5 mm diameter.

**Collimation** Simulations were performed at 10 m and 5 m collimation. In the case of 5 m collimation, the rear detector was moved forward to 5 m from the sample.

The virtual sample used was of elastic scattering from 1 mm of water.

All simulations have been performed using the "Window Frame" detector layout as sufficiently detailed simulations of the "Lined Tube" style detector are still ongoing and will be used during the initial engineering phase to determine the best detector layout. The detector efficiency was assumed to be 100% at all wavelengths. Whilst this is unlikely to be the case, it is a good approximation to the detector used at D22 and so is a reasonable comparison and we aim to design our detectors for high efficiency at all wavelengths.

Table 3.4 gives the flux on sample and minimum accessible Q as a function of sample aperture and wavelength range and figures 3.14 - 3.16 show the count rate as a function of Q for various configurations of the instrument. Equivalent configurations of D22 were also simulated using the McStas mode kindly provided by E. Farhi at the ILL and are show in the figures along with the LoKI results.

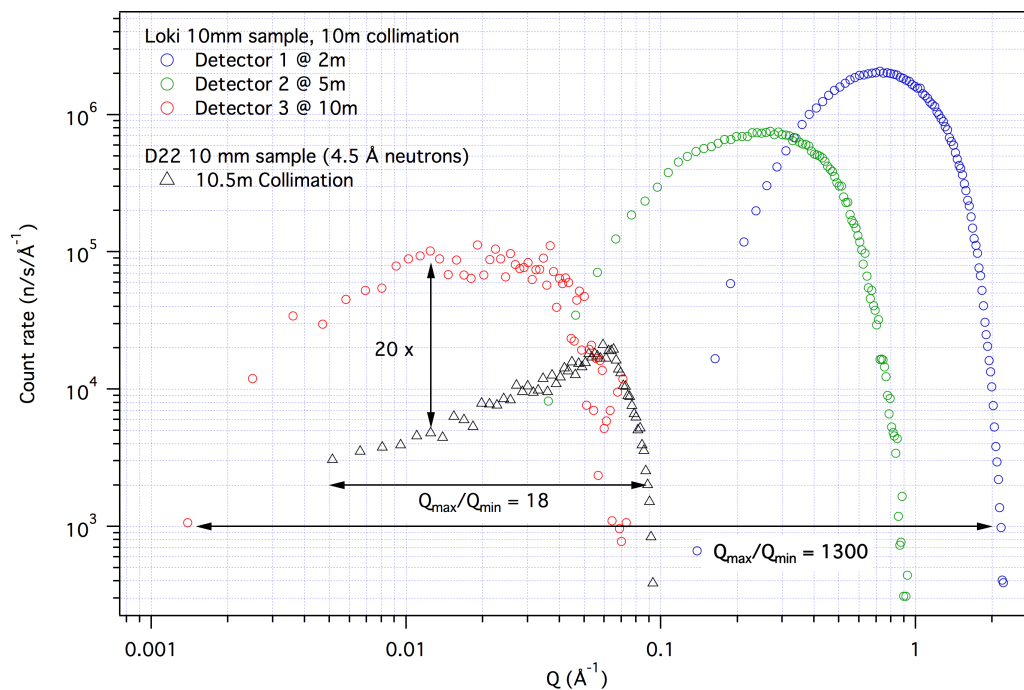


Figure 3.14: Simulated elastic scattering from a 10mm diameter  $\times$  1mm thick sample of H<sub>2</sub>O on LoKI with 10m collimation and on D22 with 10.5m collimation and 4.5 Å neutrons.

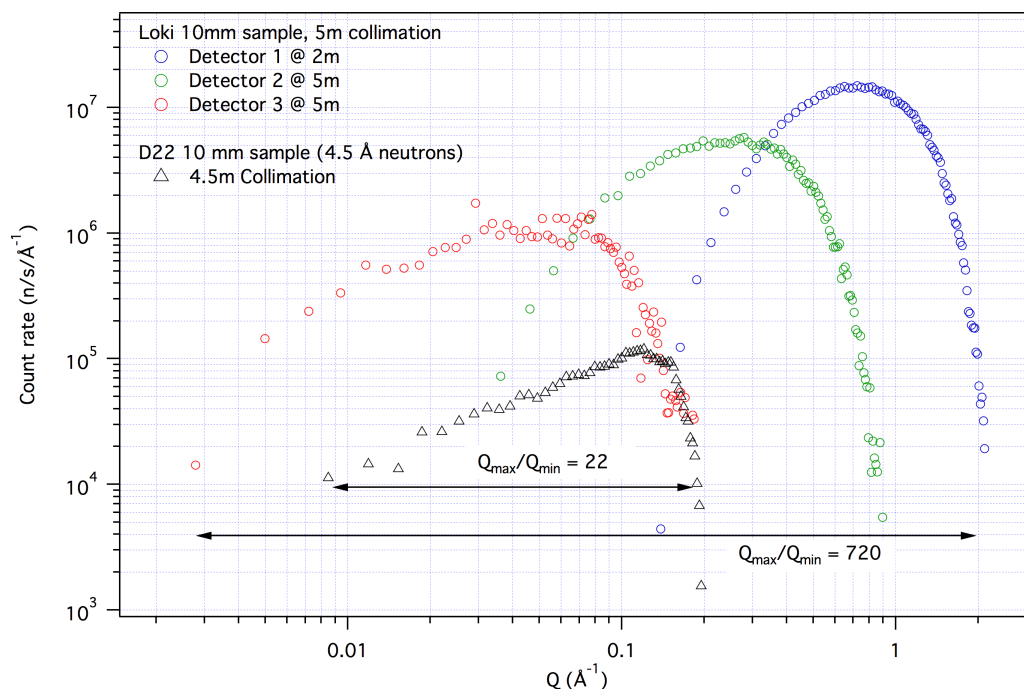


Figure 3.15: Simulated elastic scattering from a 10mm diameter  $\times$  1mm thick sample of H<sub>2</sub>O on LoKI with 5m collimation and on D22 with 4.5m collimation and 4.5 Å neutrons.

Ap2 Diam (mm)	L1 (m)	$Q_{min} (\times 10^{-3} \text{ \AA}^{-1})$	Flux (n/cm <sup>2</sup> /s)	Current (n/s)
10	2	7.63	7.64E+08	9.73E+08
5	2	3.82	4.78E+07	2.43E+08
2	2	1.53	1.22E+06	3.89E+07
10	5	3.59	1.44E+08	1.84E+08
5	5	1.79	9.03E+06	4.60E+07
2	5	0.72	2.31E+05	7.35E+06
10	10	1.79	3.98E+07	5.07E+07
5	10	0.90	2.49E+06	1.27E+07
2	10	0.36	6.37E+04	2.03E+06

Table 3.4: Flux and current on sample and minimum Q as a function of sample aperture size and collimation

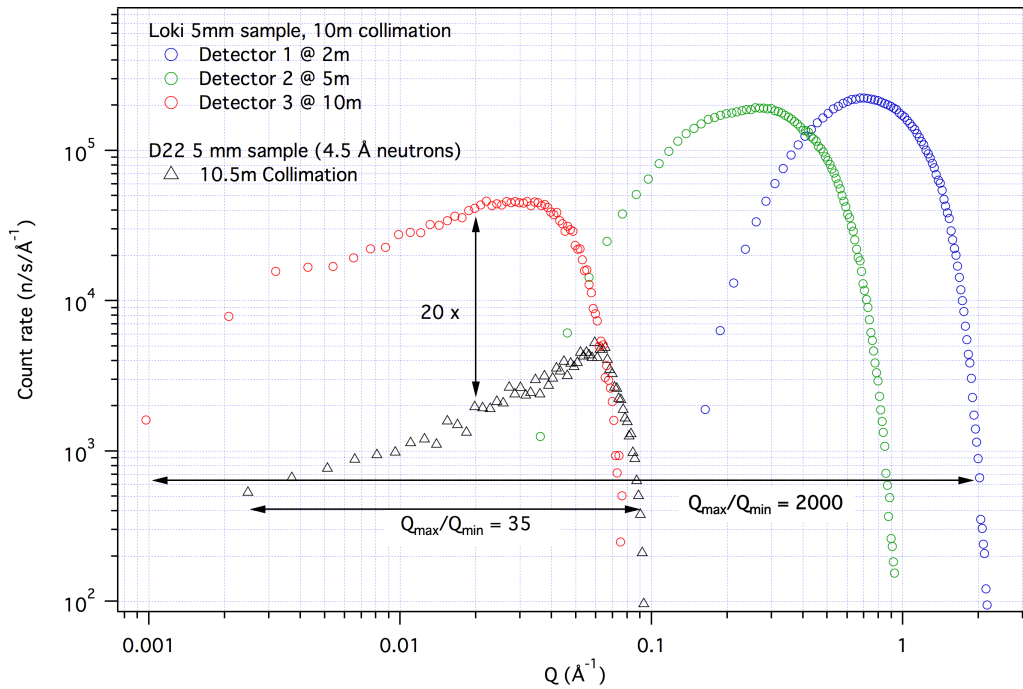


Figure 3.16: Simulated elastic scattering from a 5mm diameter  $\times$  1mm thick sample of H<sub>2</sub>O on LoKI with 10m collimation and on D22 with 10.5m collimation and 4.5 Å neutrons.





## 4 Strategy and Uniqueness

As discussed in sections 1 and 2, SANS is a technique with broad applicability that is in high demand. In order to provide for the whole science case in terms of demand, three SANS instruments should be constructed at the ESS. This is comparable to other major neutron scattering centres (NIST will soon have 4 SANS instruments and 1 USANS, ILL has 3 SANS instruments and a USANS instrument, and there are 4 SANS located at FRM II). Within Europe, the instruments most similar to LoKI are D33 at ILL (currently in commissioning) and SANS2D at ISIS, whilst D22 at ILL is widely considered to be the world-leading SANS instrument.

Once multiple instruments are required to meet demand, it makes sense to optimise each for different segments of the scientific community in order to maximise the overall impact of the suite. In order to cover the huge range of science that SANS can address in the most effective fashion the strategy for SANS at ESS calls for three instruments:

**Broad Band Small Sample SANS** Aimed at the soft matter, biophysics and materials science communities, with a wide simultaneous Q range at least 3 orders of magnitude in Q through the use of large area of detectors and wide wavelength band. Designed to maximize use of integrated intensity at cost of lower resolution.

**General Purpose Polarized SANS** Aimed at hard matter and industrial process studies, with a flexible sample area, flexible optics, polarization and polarization analysis. Multiple detector banks for at least 2 orders of magnitude simultaneous Q range. High resolution, with options for GISANS and VSANS.

**High Throughput / BioSANS** Aimed at the structural biology community, being a compact instrument with a biologically relevant length scale. Optimized for small samples and high throughput (e.g. flow through cells), it should have end-to-end automated processing and initial analysis of data (cf BioSAXS beamlines).

The first of these is represented by the instrument discussed here, LoKI. An example of the second is the work of the German SANS work package at Jülich and an example of the last is the work of the Swiss-Danish SANS work package.

The order of construction should be as listed in order to build the two instruments with the broadest applicability first. LoKI, as the broad band small sample SANS instrument, should be constructed first as there is greater scope for a new user community to be built around an instrument with high flux and a very wide simultaneous Q range as discussed in section 2.

Furthermore, the benefits of a dedicated BioSANS instrument will be achieved by fitting automated sample handling equipment to LoKI and having dedicated periods of operation for biological scattering experiments where the instrument would be operated only in one configuration. The requirements of the biological community for automated data reduction and analysis will also be of interest outside that field and so should be developed for all beamlines.

LoKI offers a world-leading combination of flux and simultaneous Q range and will be uniquely placed to deliver high impact publications in soft matter, materials science and bioscience.



## 5 Technical Maturity

SANS is a well-established technique, and time-of-flight SANS instruments have been in operation for over 20 years. This instrument has no significantly out of the ordinary components other than the detector, and there the demands on the technology are not infeasible. The combination of these components means that a world-leading instrument can be built with low technical risk.

### 5.1 Location

In order to mount and manage the complex sample environments that will be used on this instrument as well as change samples, side access to the sample area will be required. This suggests that an outside edge position on one of the 4 sectors is preferred. To minimise the background, a position facing backwards from the target (i.e. on the proton beam incoming side of the target) is preferred. However, the outside position closest to the incoming proton beam is not favoured due to space constraints and the risk of background from the proton beam scraper.

The length of the instrument and the space required for the sample position, the detector vessel and associated shielding means that two 5 degree segments from the monolith will be required, thus blocking one beamport in addition to the one used by the instrument. The location of the instrument to the left or right of the proton beam will have implications as a result of those locations having different beam heights. Whilst the lined tube style detector is relatively compact and so does not need a lot space, the window frame style detectors need at least 2.5 m from the beam centre to the floor in order to fit in the 3 m high detector bank and the rails for the detector tank to move. Furthermore, in order to accommodate the necessary sample environment equipment and associated rotation and translation stages and goniometers, a beam height of at least 2 m above the floor is required.

In the currently envisaged beam hall layout, these requirements suggest that the instrument be located in the hall with a beam height of 3 m that is facing back from the target. However, it is envisaged that this will be the "magnet free" hall to allow for operation of any spin-echo spectrometers. It is, at this stage, unclear what "magnet free" will mean in practice, but it is assumed that low-field electromagnets will be possible.

### 5.2 Risk Management

The instrument is largely based on existing technology and contains relatively few components, so the overall technological risk is low. The risks associated with some specific parts of the instrument are discussed here.

There are also generic schedule risks associated with the overall progress of the ESS construction project, but they are not considered here, as they do not affect either the scope or budget proposed.

#### Shielding

There is a great deal of uncertainty about the high-energy background that will be created by the ESS source. Low instrumental background is essential for the sorts of measurements that this instrument will be aiming to make possible. The instrument design attempts to mitigate some of this risk by avoiding direct line of sight to the moderator, however it is not clear what degree of shielding of the detectors will be required. The impact of inadequate detector

shielding would be severe given the proximity of the instrument to the target. More shielding resulting in greater cost can mitigate this risk.

Simulations of the radiation emitted from the target monolith and along the guides are in progress at the ESS and during the initial engineering design phase the instrument support divisions will work to accurately design the shielding to the needs of the instrument.

The relatively open "optics hutch" envisaged between the common shielding bunker and the sample position is a possible risk for increased background. This will be taken into account during the shielding design process, and can be mitigated by filling the space with shielding. This might, of course, remove the option of having focussing optics or SESANS.

### **Beam Delivery System**

There are risks associated with the use of high m-value guide coatings close to the target. It is possible that the coatings, if deposited on borofloat glass, will degrade rapidly in the high radiation environment, thus affecting instrument performance, as fewer neutrons will be delivered. The chance of this is moderate, but the impact would be high. Choosing lower m-value coatings can mitigate this risk, albeit at a loss of performance, but this would be a performance that would not degrade over time.

The ESS optics group has determined that this risk will be adequately mitigated through the use of substrates that do not contain boron. The most likely candidates are metal substrates or "Zerodur" ceramic substrates.

### **Detectors**

The detector systems represent the largest technological risk in this proposal. Two possible detector layouts using a mixture of detector technologies are proposed.

#### **Lined Tube**

The "lined tube" detector system is based around the use of  $^{10}\text{B}$  thin films at a grazing incidence angle. This represents a moderate development risk as such a detector has not been used for neutron scattering before and such detectors are not yet available. However, the ESS is putting significant effort and resources into these technologies and rapid progress is being made.

#### **Window Frame**

The use of  $^3\text{He}$  detectors for the first two banks whilst of low risk in development terms, represents a high risk in terms of availability of supply. A relatively large area (14 m<sup>2</sup> in the "window frame" configuration) of detectors is required and supplying this with  $^3\text{He}$  could be challenging. There are also questions about the ability of helium detectors to cope with the possible counting rate.

The alternative detector choice for that large area is  $^{10}\text{B}$  thin film based technology, either inclined blades or stacked layers depending on the required resolution. This represents a moderate development risk as such detectors are not yet available in large areas.

#### **High-resolution low angle detector**

In either of the detector layouts presented, the low angle detector at the rear is based on scintillator technology, such as Anger cameras or wavelength-shifting fibres. Such detectors are currently in use at other facilities and are well understood. As such this does not represent

a significant risk. There are questions as to the count rate capacity of such detectors but with the pace of detector development, it is anticipated that alternatives will be available.

In all cases, any detector design that requires research and development work carries a schedule risk. It is possible that the necessary detectors will prove more complex to develop than envisaged, or that the capacity to manufacture sufficient detectors in a timely fashion will not be available. This risk can be mitigated by increased allocation of resources by the ESS instrument support division to the detector group. Furthermore, in the case of either of the detector layouts, detectors can be installed as they become available over the commissioning period, thus diminishing the schedule risk at the cost of lower initial performance.

### **Supporting Facilities**

The availability of excellent sample environment equipment, sufficient laboratory space for sample handling and preparation, and non-neutron characterisation equipment will be vital to achieving the full potential of this instrument. If the ESS does not provide for these needs then the high performance of the instrument will not be fully utilised and research impact will be weakened.



## 6 Costing

Three different options are presented for the detectors as discussed in section 3.6, namely the lined tube with  $^{10}\text{B}$ , window frames with  $^3\text{He}$  and window frames with  $^{10}\text{B}$ . In all cases the high-resolution low angle detector at the rear is based on Anger cameras. All cases include the cost of an instrumented beam stop that can provide a time-of-flight spectrum.

**Window frames with  $^3\text{He}$**  14 m<sup>2</sup> of 8 mm  $^3\text{He}$  tubes.

Total cost = 19.6 M

**Window frames with  $^{10}\text{B}$**  14 m<sup>2</sup> of 8 mm pitch  $^{10}\text{B}$  multi-layer detectors.

Assumes detector cells 15 layers deep such that the total area of coating is  $\sim 200\text{ m}^2$

Total cost = 14.2 M

**Lined Tube with  $^{10}\text{B}$**  34 m<sup>2</sup> of 5 cm pitch  $^{10}\text{B}$  inclined geometry detectors.

Assumes detector cells on average 2 layers deep (optimisation of number of layers by distance has not yet been done) such that the total area of coating is  $\sim 70\text{ m}^2$ . This costing includes readout channels in both directions to improve azimuthal resolution.

Total cost = 11.6 M

If the cost of instrument control, data reduction and data analysis software development and deployment is included then the cost of the instrument is increased by 720 k based on 6 person-years of effort over the project, assuming some common development with other instruments.

The costing is presented in more details in tables below and is broken down into the four phases of the instrument construction project. The staff effort is estimated in person-months assuming a cost of 10 k/person-month. The costs are also broken down into the following categories:

**Integrated Design** The effort from the Lead Scientist and engineer, as well as other scientists and engineers involved in the overall instrument design

**Systems Integration** Systems engineering activities to ensure compatibility between components and compliance with ESS standards.

**Detectors and Data Acquisition** Detector systems complete with all electronics. The cost estimates are based on discussions with the ESS Detector group and hardware costs include installation.

**Optical Components** The beam delivery system including the bender, guide, the guide housing and alignment system and collimation slits. The cost estimates are based on a confidential market survey by the ESS Neutron Optics group. The hardware costs include installation.

**Choppers** The chopper systems for bandwidth selection and frame overlap suppression

**Detector Vessel** The vacuum vessel for the detectors, including pumps, windows, mounting and installation. Sample Environment: The necessary goniometers, rotation and translation stages for mounting sample environment and necessary SANS specific sample environment such as a Rheometer, sample changers, flow cell, electromagnet etc.

**Shielding** The shielding solutions required for radiation protection and background reduction, including shutter systems. The requirements and costing model for the shielding is unclear at the moment, so the current estimate is an engineering estimate from the ESS Neutron Optics group.

**Instrument Specific Support Equipment** This includes mechanical components not costed elsewhere. Instrument Infrastructure: The buildings and facilities not provided as part of the Conventional Facilities budget, such as cabins, mezzanines, raised floor areas etc. As no definite floor plan exists at the moment, the estimate here is based on information from SNS and ISIS.

The majority of the costs are incurred in the Procurement and Installation phase, but some of the major procurements could be initiated in the Final Design phase at the discretion of the Chief Instrument Engineer.

This cost estimate should be regarded as very preliminary and indicative of the relative cost profile between the various components. The uncertainty in the cost estimates will be significantly reduced once a preliminary engineering design is available.



in k€	Phase 1 (Design and Planning)			Phase 2 (Final Design)			Phase 3 (Procurement and Installation)			Phase 4 (Beam Testing and Cold Commissioning)			Total		
	Hardware	Staff (k€)	Staff (months)	Hardware	Staff (k€)	Staff (months)	Hardware	Staff (k€)	Staff (months)	Hardware	Staff (k€)	Staff (months)	Hardware	Staff (k€)	Staff (months)
Integrated Design	0	360	36	0	600	60	0	480	48	0	240	24	0	1680	168
Systems Integration	0	0	0	0	30	3	0	120	12	0	60	6	0	210	21
Detectors and Data Acquisition	0	30	3	0	30	3	11500	60	6	200	120	12	11700	240	24
Optical Components	0	30	3	0	30	3	500	30	3	20	60	6	520	150	15
Choppers	0	30	3	0	30	3	250	30	3	20	30	3	270	120	12
Detector Vessel	0	30	3	0	30	3	1500	30	3	0	10	1	1500	100	10
Sample Environment	0	0	0	0	30	3	500	10	1	200	60	6	700	100	10
Shielding	0	30	3	0	60	6	1500	60	6	20	60	6	1520	210	21
Instrument Specific Support Equipment	0	0	0	0	30	3	100	120	12	20	30	3	120	180	18
Instrument Infrastructure	0	30	3	0	30	3	100	60	6	20	30	3	120	150	15
Total	0	540	54	0	900	90	15950	1000	100	500	700	70	16450	3140	314
<b>Grand total (no VAT)</b>								<b>19590</b>							

Figure 6.1: Costing for LoKI with “window frame” style detectors using  $^3\text{He}$

in k€	Phase 1 (Design and Planning)			Phase 2 (Final Design)			Phase 3 (Procurement and Installation)			Phase 4 (Beam Testing and Cold Commissioning)			Total			
	Hardware	Staff (k€)	Staff (months)	Hardware	Staff (k€)	Staff (months)	Hardware	Staff (k€)	Staff (months)	Hardware	Staff (k€)	Staff (months)	Hardware	Staff (k€)	Staff (months)	Staff (years)
Integrated Design	0	360	36	0	600	60	0	480	48	0	240	24	0	1680	168	14.00
Systems Integration	0	0	0	0	30	3	0	120	12	0	60	6	0	210	21	1.75
Detectors and Data Acquisition	0	30	3	0	30	3	6000	60	6	200	120	12	6200	240	24	2.00
Optical Components	0	30	3	0	30	3	500	30	3	20	60	6	520	150	15	1.25
Choppers	0	30	3	0	30	3	250	30	3	20	30	3	270	120	12	1.00
Detector Vessel	0	30	3	0	30	3	1500	30	3	0	10	1	1500	100	10	0.83
Sample Environment	0	0	0	0	30	3	500	10	1	200	60	6	700	100	10	0.83
Shielding	0	30	3	0	60	6	1500	60	6	20	60	6	1520	210	21	1.75
Instrument Specific Support Equipment	0	0	0	0	30	3	100	120	12	20	30	3	120	180	18	1.50
Instrument Infrastructure	0	30	3	0	30	3	100	60	6	20	30	3	120	150	15	1.25
Total	0	540	54	0	900	90	10450	1000	100	500	700	70	10950	3140	314	26.17
<b>Grand total (no VAT)</b>														<b>14090</b>		

Figure 6.2: Costing for LOKI with “window frame” style detectors using <sup>10</sup>B

in k€	Phase 1 (Design and Planning)			Phase 2 (Final Design)			Phase 3 (Procurement and Installation)			Phase 4 (Beam Testing and Cold Commissioning)			Total		
	Hardware	Staff (k€)	Staff (months)	Hardware	Staff (k€)	Staff (months)	Hardware	Staff (k€)	Staff (months)	Hardware	Staff (k€)	Staff (months)	Hardware	Staff (k€)	Staff (months)
Integrated Design	0	360	36	0	600	60	0	480	48	0	240	24	0	1680	168
Systems Integration	0	0	0	0	30	3	0	120	12	0	60	6	0	210	21
Detectors and Data Acquisition	0	30	3	0	30	3	4000	60	6	200	120	12	4200	240	24
Optical Components	0	30	3	0	30	3	500	30	3	20	60	6	520	150	15
Choppers	0	30	3	0	30	3	250	30	3	20	30	3	270	120	12
Detector Vessel	0	30	3	0	30	3	1000	30	3	0	10	1	1000	100	10
Sample Environment	0	0	0	0	30	3	500	10	1	200	60	6	700	100	10
Shielding	0	30	3	0	60	6	1500	60	6	20	60	6	1520	210	21
Instrument Specific Support Equipment	0	0	0	0	30	3	100	120	12	20	30	3	120	180	18
Instrument Infrastructure	0	30	3	0	30	3	100	60	6	20	30	3	120	150	15
Total	0	540	54	0	900	90	7950	1000	100	500	700	70	8450	3140	314
<b>Grand total (no VAT)</b>														<b>11590</b>	

Figure 6.3: Costing for LoKI with "lined tube" <sup>10</sup>B detectors